

# We are IntechOpen, the world's leading publisher of Open Access books Built by scientists, for scientists

4,800

Open access books available

122,000

International authors and editors

135M

Downloads

Our authors are among the

154

Countries delivered to

TOP 1%

most cited scientists

12.2%

Contributors from top 500 universities



WEB OF SCIENCE™

Selection of our books indexed in the Book Citation Index  
in Web of Science™ Core Collection (BKCI)

Interested in publishing with us?  
Contact [book.department@intechopen.com](mailto:book.department@intechopen.com)

Numbers displayed above are based on latest data collected.  
For more information visit [www.intechopen.com](http://www.intechopen.com)



---

# Superalloys for Advanced Ultra-Super-Critical Fossil Power Plant Application

---

Xishan Xie, Yunsheng Wu, Chengyu Chi and Maicang Zhang

Additional information is available at the end of the chapter

<http://dx.doi.org/10.5772/61139>

---

## Abstract

Superalloys are world-wildly used not only for aerospace but also for chemistry, oil & gas and power engineering application. In recent years the 700 °C level Advanced Ultra-Super-Critical (A-USC) technology with high thermal efficiency is developing in the world to reduce the coal consumption and pollution emissions. Any kind of advanced ferritic and austenitic heat-resisting steels can not meet 700 °C A-USC technology requirement. In this case high quality Ni-base superalloys must be adopted for 700 °C A-USC technology. The research and development of Ni-Fe and Ni-base superalloys such as HR6W, GH2984, Haynes 230, Inconel 617/617B, Nimonic 263, Haynes 282, Inconel 740 and 740H are reviewed in this chapter.

**Keywords:** Ni-base superalloys, A-USC power plant, Long time aging, Stress-rupture strength, Structure stability

---

## 1. Introduction

Superalloys are world-wildly used not only for aerospace but also for chemistry, oil & gas and power engineering application.

Electricity is one of the most important pillars for mankind living and economic development. Most of the countries in the world electricity is generated by coal fired power plants. In half of the century steam temperatures of coal fired power plants are going up from 475 °C to 600 °C. In this temperature range heat-resisting steels such as ferritic and austenitic steels are

wildly used. Recently for further raising thermal efficiency and reduction of CO<sub>2</sub> emission the 700 °C advanced ultra-super-critical (A-USC) power plant development projects are initiated in Europe, United States, Japan, China and India also. In 700 °C A-USC project the highest temperature parts are boiler super-heater and re-heater tube components. The fire-side metal temperature of these components can reach 750-760 °C even higher. Today’s modern power plants are required for very long time service such as 30-40 years. There are very strict requirements of these high temperature tube materials such as:

1. The high temperature stress rupture strength for 10<sup>5</sup> h should be higher than 100 MPa;
2. The fire-side metal oxidation layer after 10<sup>5</sup> h should be less than 1 mm;
3. Good structure stability at long time service and no harmful phase formation;
4. Good process performance such as fabrication and welding ability etc.

At above mentioned serious condition any kind of ferritic and austenitic heat-resisting steels can not fulfill these requirements. The high quality Ni-base superalloys must be used for A-USC power plant application. Figure\_1 clearly shows the ratio change of high temperature materials with the steam parameters development for coal fired power plants. The Ni-base superalloys will occupy 29% for a 360 bar/700 °C/720 °C A-USC power plant [1].

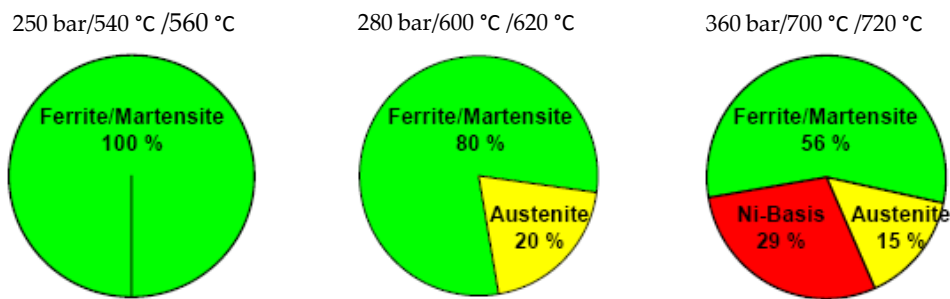


Figure 1. The ratio change of high temperature materials with the steam parameters development for coal fired power plants.

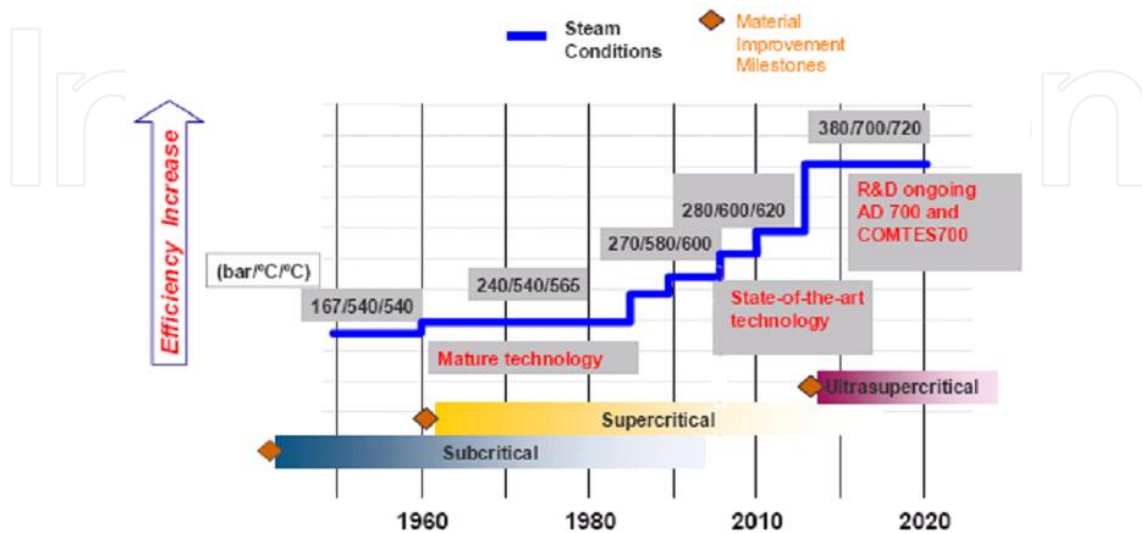


Figure 2. The steam parameters development of coal fired power plants in the world.

Figure 2 shows the steam parameters development of coal fired power plants in the world [2]. Now the “bottle neck” issue is adopting high performance long life superalloys. The European Union initiated their 700 °C A-USC Project from the year of 1998. Up to now they have not got successful results because of the failure of Ni-base alloy weldment at their test bed.

The purpose of this chapter is to give an overview of today’s Ni-base superalloys for high temperature (700 °C even higher) A-USC power plant materials selection and application.

## 2. Superalloys for 700°C A-USC power plant

The nominal chemical compositions of candidate Ni-Fe and Ni-base superalloys for 700 °C A-USC power plant are shown in Table 1. The alloys of HR6W (developed by Sumitomo Metal, Japan) and GH2984 (developed by Institute of Metal, China) are Ni-Fe base superalloys. The others are Ni-base superalloys developed by Haynes and Special Metals Corp. (formerly INCO Alloys International, USA).

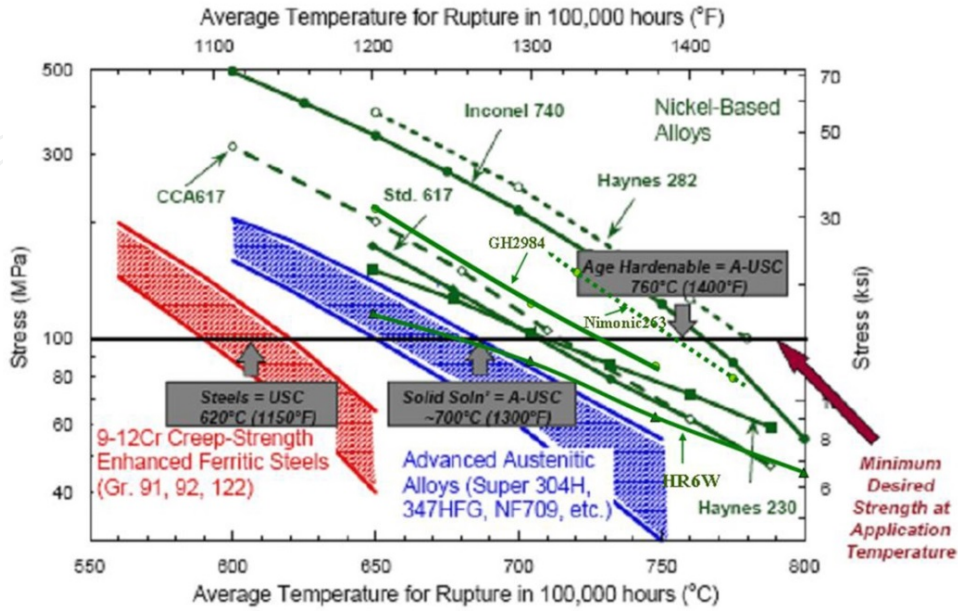
Alloy	ASME Code	C	Cr	Co	Mo	Nb	Ti	Al	Si	Mn	Fe	W	Cu	Ni
HR6W	2684	0.08	23	-	-	0.2	0.1	-	0.5	1.0	Bal.	7	-	45
GH2984	No	0.06	19	-	2.2	1.1	1.1	0.4	≤0.5	≤0.5	33	-	-	Bal.
Haynes230	2063	0.10	22	≤5	2.0	-	-	0.3	0.4	0.5	≤3	14	0.02(La)	Bal.
Inconel 617B	2439	0.06	22	12	9.0	-	0.4	1.0	≤1.0	≤1.0	≤1.5	-	-	Bal.
Haynes282	No	0.06	20	10	8.5	-	2.1	1.5	≤0.15	≤0.3	≤1.5	-	-	Bal.
Nimonic263	No	0.06	20	20	6.0	-	2.2	≤0.6	≤0.4	≤0.6	≤0.7	-	≤0.2	Bal.
Inconel740	2702	0.03	25	20	0.5	2.0	1.8	0.9	0.5	0.3	≤0.7	-	-	Bal.
Inconel740H	2702	0.03	25	20	0.5	1.5	1.35	1.35	0.15	0.3	≤0.7	-	-	Bal.

**Table 1.** Nominal chemical compositions (wt %) of candidate high temperature materials for 700 °C A-USC power plant.

HR6W and GH2984 are based on Ni-Fe-Cr austenite matrix and solid solution strengthened by Mo and W and also precipitation strengthened by Nb, Ti and Al. Most of Ni-base superalloys are based on Ni-Cr-Co austenite matrix with solid solution strengthening by molybdenum (0.5%-9%Mo) and  $\gamma'$  precipitation strengthening by adding Ti, Al and Nb also. Haynes 230 is mainly a solid solution strengthening Ni-base superalloy strengthened by Cr, W and Mo.

The creep strengths for 10<sup>5</sup> h at different temperatures of above mentioned high temperature materials are shown in Figure\_3 [3-6]. Inside temperatures of superheater and reheater tube loops for 700 °C/720 °C A-USC boiler are 700 and 720 °C respectively. However the fireside temperature of these tubes can reach 760 °C even higher. The arrow indication at the 100MPa margin is critical for 700 °C/720 °C A-USC boiler tube materials selection. From point of view on this critical margin only Inconel 740 Ni-base superalloy is acceptable. It seems to us that

Haynes 282 may characterize with the highest creep strength among these candidate materials. However Haynes 282 is still under the developing for superheater and reheater tube products and also have not been issued ASME code.



(R. Romanosky, 2011; J.T. Guo, 2005; H. Semba, 2008; X.S. Xie, 2013)

Figure 3. Creep strength comparison among some candidate materials.

The fireside coal ash corrosion is also a critical criterium for 700 °C A-USC boiler superheater and reheater tube selection. Figure\_4 shows a complete series results of different high temperature materials [7]. It is clearly shown that high contents of Mo and W are harmful for coal ash corrosion. Inconel 740 with very low content of Mo (0.5% Mo only) characterizes with excellent coal ash resistance (as the star indicated in Figure\_4).

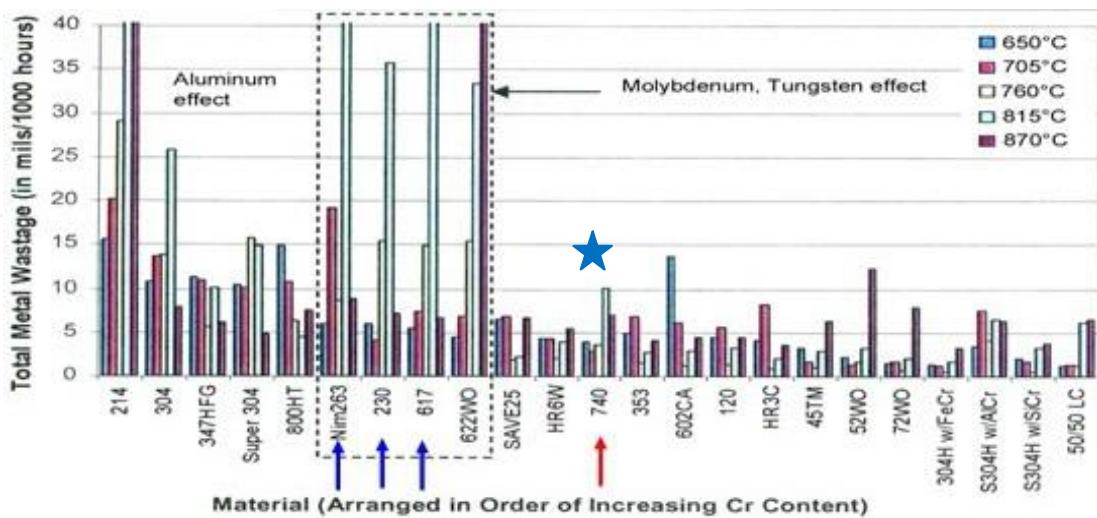


Figure 4. Coal ash corrosion of some candidate materials.

### 2.1. HR6W (45Ni-Fe-23Cr-7W-0.2Nb-0.1Ti-0.08C)

HR6W is a Ni-Fe base superalloy mainly strengthening by 7%W which was developed by Sumitomo Metals, Japan in 1986. The large amount of W is not only for solid solution strengthening but also for precipitation strengthening of Laves phase. According to the thermodynamic calculated phase diagram (Figure\_5) the main precipitated phase is Laves phase and also  $M_{23}C_6$ , M(C, N) and  $\alpha$ -Cr formation at 700 °C. A small amount of B addition in HR6W is for grain boundary strengthening [8].

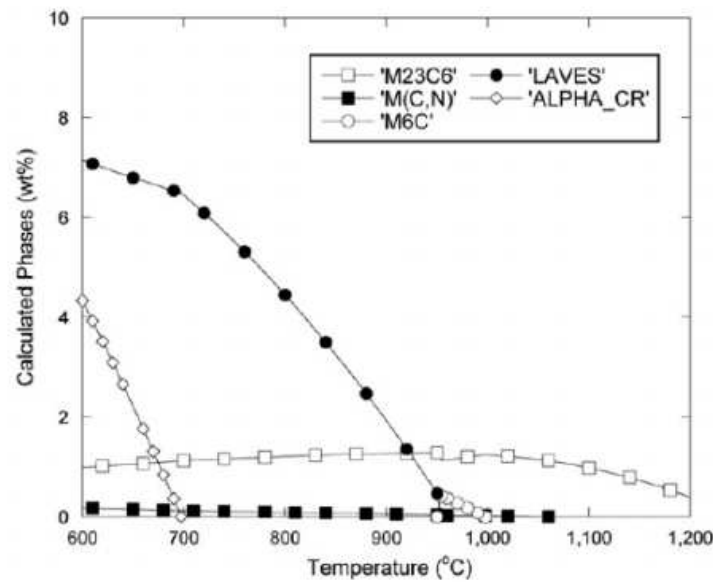


Figure 5. The calculated thermodynamic equilibrium phase diagram of HR6W alloy.

The fraction of main strengthening phase Laves is dramatically increased with the W content (from 3% to 8%), but there is almost no influence on  $M_{23}C_6$  and MX phases (Figure\_6a). However the fraction of  $\alpha$ -Cr is dramatically increased when the Cr is higher than 23.4% (Figure\_6b) [8].

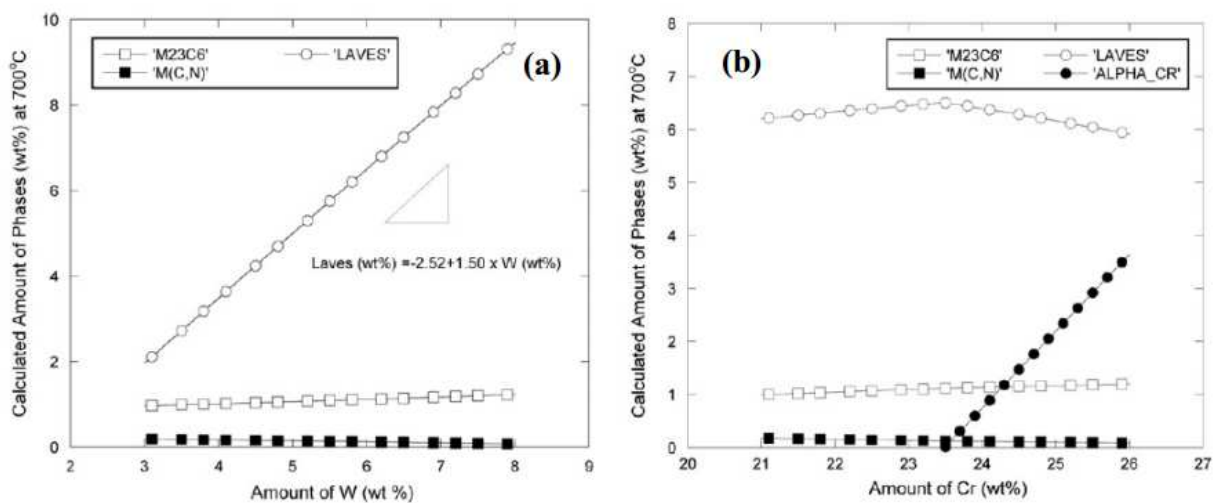
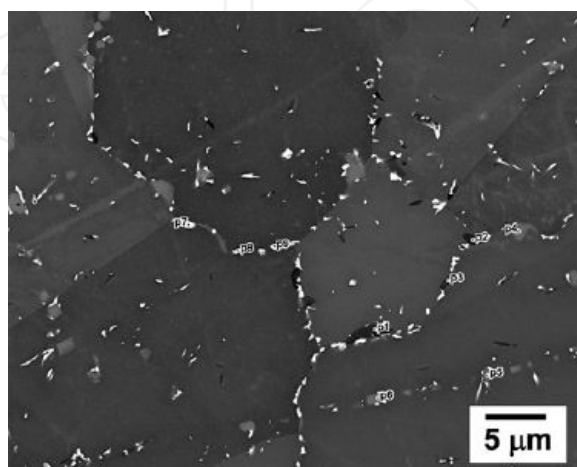


Figure 6. The calculated amount of equilibrium phases at 700 °C in HR6W alloy change with W (a) and Cr (b).



Tungsten is concentrated in Laves phase and the Cr diffuse away from Laves phase to the interphase of Laves/ $\gamma$  matrix. In result of that the concentration of Cr promotes  $\alpha$ -Cr formation. Figure\_7 shows  $\alpha$ -Cr particles with Laves phase at grain boundaries and also in the grains at the vicinity of Laves phase [8].



**Figure 7.** The EBSD picture of HR6W alloy crept at 700°C/100 MPa, 7998.6 h.

TEM images (Figure\_8) clearly shows the precipitated Laves phase morphology after long time stress rupture tests at 700, 750 and 800 °C [9]. It can be seen that the growth rate of Laves phase is very sensitive to the test temperature. The dispersive precipitated Laves phase is already grown to a certain size at 750 °C after long time stress rupture test.

The stress-rupture strength of HR6W in the temperature range from 650-800 °C are shown in Figure\_9 [10]. The extrapolated stress-rupture strength for 10<sup>5</sup> h at 700 °C is 88 MPa only. It is difficult to fulfil 700 °C A-USC boiler superheater and reheater tube requirement.

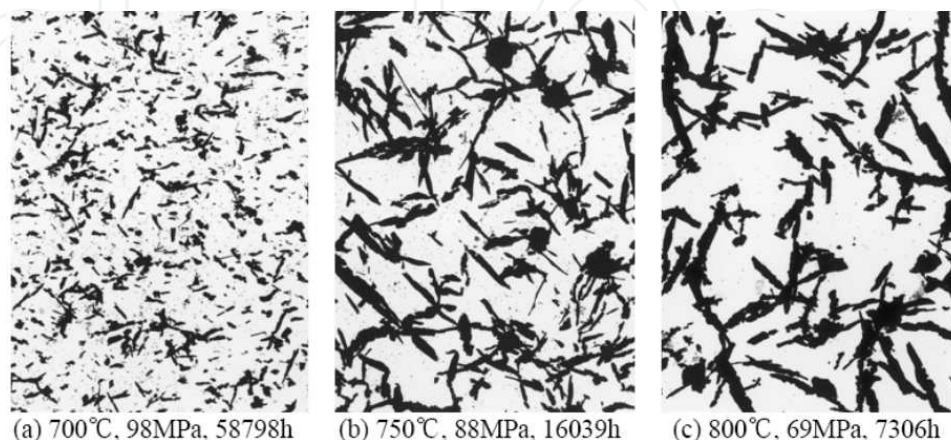


**Figure 8.** The microstructure of HR6W alloy after creep test at 700 °C (a), 750 °C (b) and 800 °C (c) respectively.

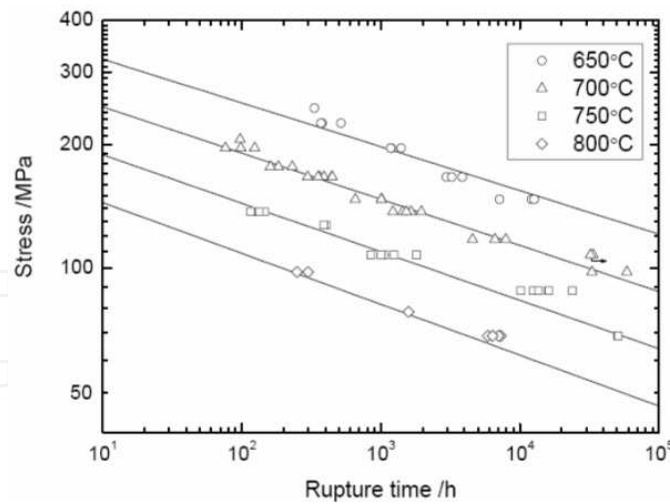


Figure 9. Stress rupture strength curves of HR6W at different temperature.

## 2.2. GH2984 (Ni-33Fe-20Cr-2Mo-1Nb-1Ti-0.35Al-0.06C)

GH2984 is a Ni-Fe base superalloy with the solid solution strengthening of big amount of Cr (20%) and small amount of Mo (2%). Certain amount of Nb, Ti, Al addition is for Ni<sub>3</sub>(Nb, Ti, Al) type  $\gamma'$  phase precipitation strengthening. GH2984 was developed by the Institute of Metal Research, China in the year of 1970'. GH2984 contains 33% Fe, which is an economic superalloy in comparison with other Ni-base superalloys. GH2984 has been used as a marine ship boiler superheater components for long term service more than 10 years [11]. It is recommended for tube components in the temperature range of 650-700 °C.

The main precipitation strengthening phase in GH2984 is  $\gamma'$ -Ni<sub>3</sub>(Nb, Ti, Al). GH2984 contains 5.74%  $\gamma'$  with the average size of 23 nm after standard heat treatment. However the brittle  $\sigma$  phase formation (about 3%) happens after long time aging at 700 °C. Except this the  $\gamma'$  growth rate is also high in the temperature range of 700-750 °C [11]. GH2984 contains 20%Cr and show good oxidation resistance. Figure\_10 shows its oxidation dynamic curves at 650 and 700 °C [12]. The average oxidation rate at 700 °C for 100h is 0.0058 g/m<sup>2</sup> h only.

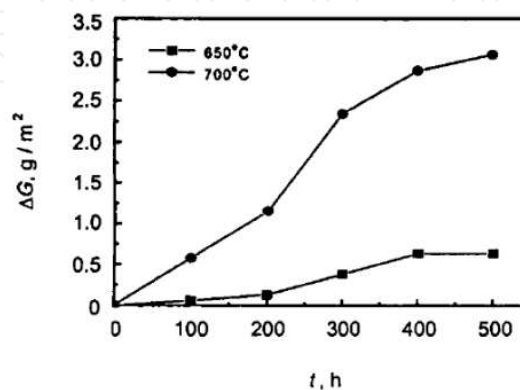


Figure 10. The oxidation curves of GH2984 alloy at 650 and 700 °C.



Careful control of the main  $\gamma'$  strengthening elements Nb, Ti and Al is important for GH2984. The optimum contents of these  $\gamma'$  strengthening elements are recommended as 1.35%Nb, 1.24%Ti and 0.65%Al [13]. The stress rupture strength curves of GH2984 in the temperature range of 650-800 °C are shown in Figure\_11 [5]. Because of the low fraction of  $\gamma'$  strengthening phase the stress rupture strength of GH2984 still can not fulfill 700 °C A-USC boiler superheater and reheater tube components requirement. Recently Institute of Metal Research, China is making the modification of GH2984 for developing GH2984G and try to fulfill the 700 °C A-USC project in China.

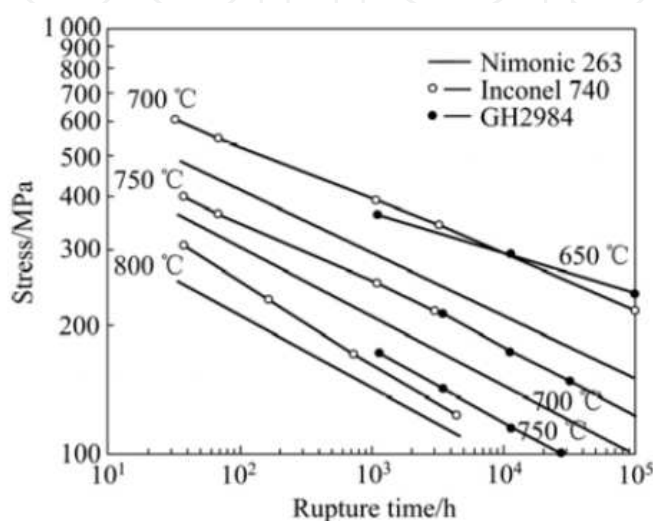


Figure 11. Stress rupture curves of GH2984 alloy in comparison with Nimonic263 and Inconel740

### 2.3. Haynes 230 (Ni-22Cr-2Mo-14W-0.3Al-0.1C-La)

Hayne 230 developed by Haynes International in 1984, is a typical solid solution strengthening Ni-base alloy with high contents of Cr (22%) and W (14%) and partially Mo (2%) [14]. Haynes 230 characterizes with good workability for hot deformation in a wide temperature range from 925 °C to 1175 °C. There are no harmful phase (such as  $\sigma$  and  $\mu$  phase) formation in the temperature range of 649-871 °C for long time aging till 16,000 h [15].

Figure\_12a shows a typical austenitic structure with the grain boundary precipitated  $M_6C$  carbide at mill annealed condition [16]. The zig-zag grain boundaries can be formed by grain boundary carbide precipitation as shown in Figure\_12b. It can block grain boundary sliding for improvement of creep resistance at high temperature.

A detail study on the strengthening mechanism of Haynes 230 shows that a fine intermetallic phase  $Ni_2(Cr, W)$  can precipitate in  $\gamma$ -matrix for improvement of creep resistance. Figure\_13 shows the precipitation of  $Ni_2(Cr, W)$  phase after 1000 h creep test at 750 °C, 28 MPa [17]. Because of the very low fraction of  $Ni_2(Cr, W)$  phase the strengthening effect is also not strong. In result of that Haynes 230 still can not meet the stress rupture strength higher than 100 MPa at 750 °C for  $10^5$  h.

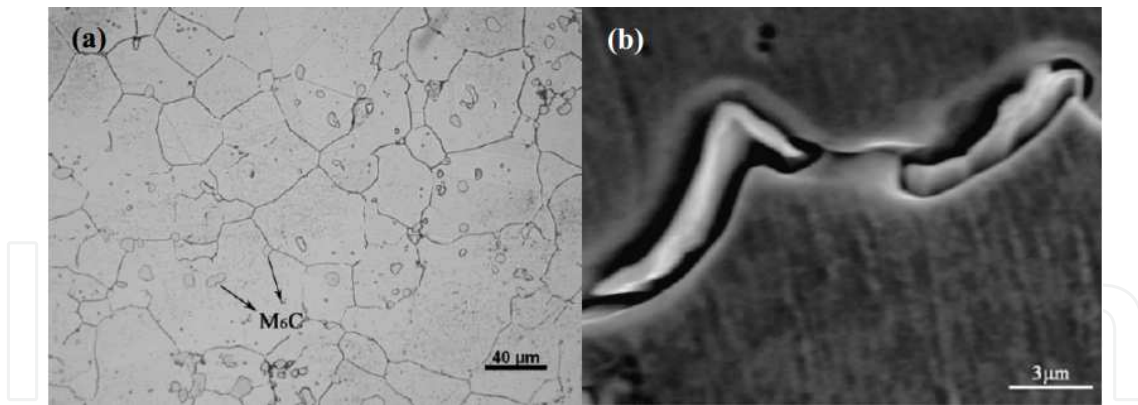


**Figure 12.** The microstructure of Haynes230 alloy at supplied condition (a) carbide precipitation at grain boundaries (b).

#### 2.4. Inconel 617/617B (Ni-22Cr-12Co-9Mo-0.4Ti-1Al-0.06C)

Inconel 617 was originally developed by INCO Alloys International in the year of 1975. It is a mainly solid solution strengthening superalloy based on Ni-Cr-Co  $\gamma$ -matrix by adding high content of Mo (9%) and also a small amount of Al and Ti for  $\gamma'$  precipitation strengthening [18]. For creep resistant improvement Alloy 617B was further developed by Thyssen-Krupp VDM, Germany for strictly control of Al and Ti contents and also boron addition for grain-boundary strengthening. Alloy 617B sometimes is also designated as 617CCA or 617Mod.

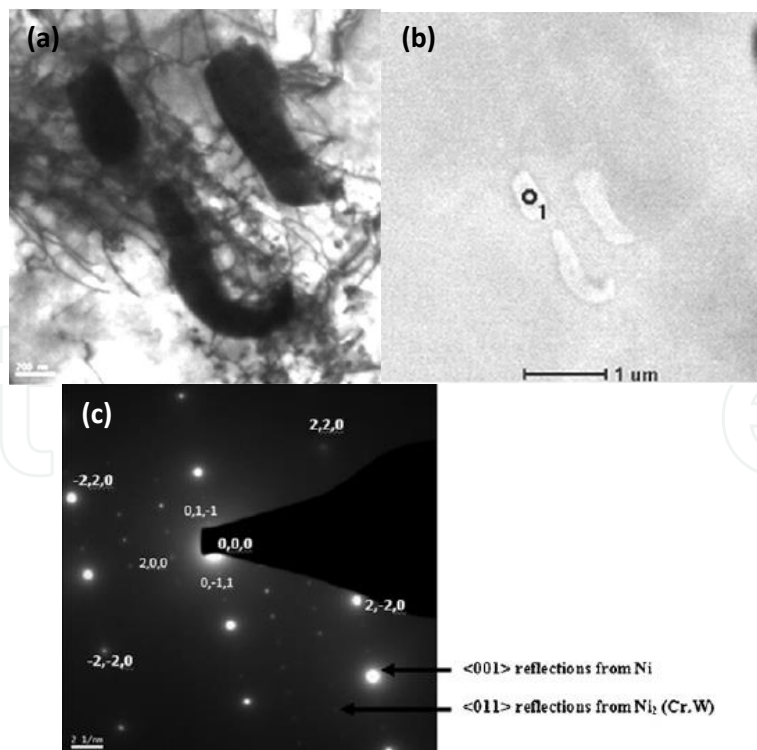


**Figure 13.** TEM (a), SEM (b) and diffraction patterns (c) of  $\text{Ni}_2(\text{Cr,W})$  in Haynes230 alloy after creep test at 750 °C /28 MPa, 1000h.

Phase diagram calculation by Thermo-Calc can help us to understand the phase stability in the different temperature ranges. As the equilibrium phase diagram of Inconel 617B (Figure\_14) shows that the  $\sigma$  and  $\mu$  phase can be formed in different temperature ranges.

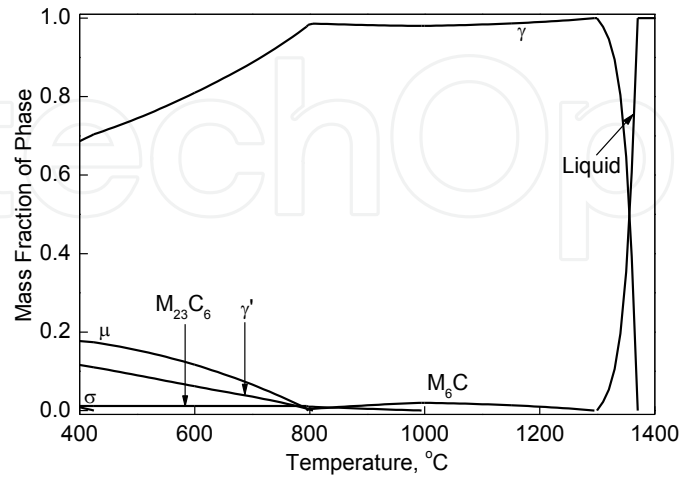


Figure 14. Phase diagram of Inconel 617B calculated by Thermo-Calc.

Quanyan Wu [19, 20] has systematically studied its microstructure behaviour in the temperature range of 482-871 °C for long time aging till 65,000 h. A group of TTT curves are shown in Figure\_15. It can be seen from this diagram that there are no  $\sigma$  and  $\mu$  phase formation. The main precipitated phases are  $\gamma'$ , MX,  $M_6C$  and  $M_{23}C_6$  [19].

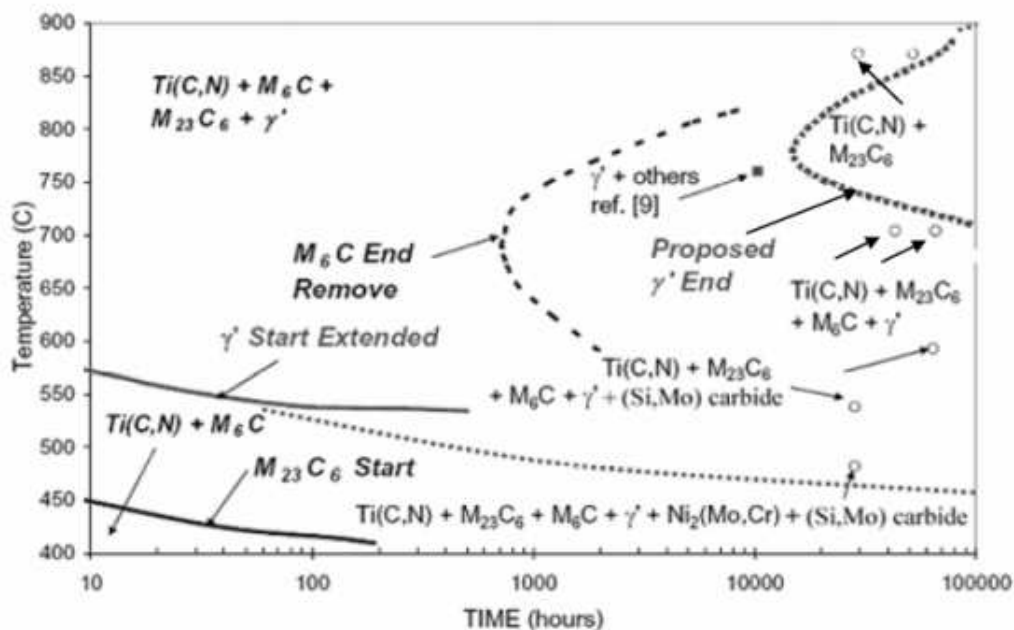


Figure 15. TTT curves of modified Inconel617 based on observation of TEM and SEM results of long-term aging samples

According to Wu's study, the average size of  $\gamma'$  after long-time aging at 704 °C for 43,100 h is about 40-60 nm, but its volume fraction is low, about 5% only. However, the size of  $\gamma'$  grows rapidly at 704 °C for 65,000 h (about 200 nm) and  $\gamma'$  volume fraction decreases to a lower level.

The  $\gamma'$  precipitation and growth behavior can be clearly seen from Figure\_16 at long-time aging for 1000 and 3000 h at 700, 750 and 800 °C. The strengthening phase  $\gamma'$  grows rapidly with increasing temperature and simultaneously  $\gamma'$  dispersion degree and its volume fraction both decrease rapidly [20].

In result of that Inconel 617/617B (617CCA or 617Mod) can not meet 700 °C A-USC project requirement as Figure\_3 indicated.

### 2.5. Nimonic 263 (Ni-20Cr-20Co-6Mo-2Ti-0.6Al-0.06C)

Nimonic 263 was originally developed by Rolls-Royce in 1971 as a high stress rupture strength and corrosion resistant Ni-base superalloy. It is based on Ni-Cr-Co austenitic matrix with high content of Mo (6%) for further solid solution strengthening. Especially 2%Ti and 0.6%Al addition to this alloy for forming about 10%  $\text{Ni}_3(\text{Al, Ti})$  type  $\gamma'$  creates good solid solution with  $\gamma'$  precipitation strengthening and also boron addition for grain boundary strengthening in a good combination for the improvement of high temperature creep resistance. As we can see in Figure\_3 that Nimonic 263 can just reach the  $10^5$  h stress rupture strength at 750 °C for 700 °C A-USC boiler superheater and reheater tubing requirement.

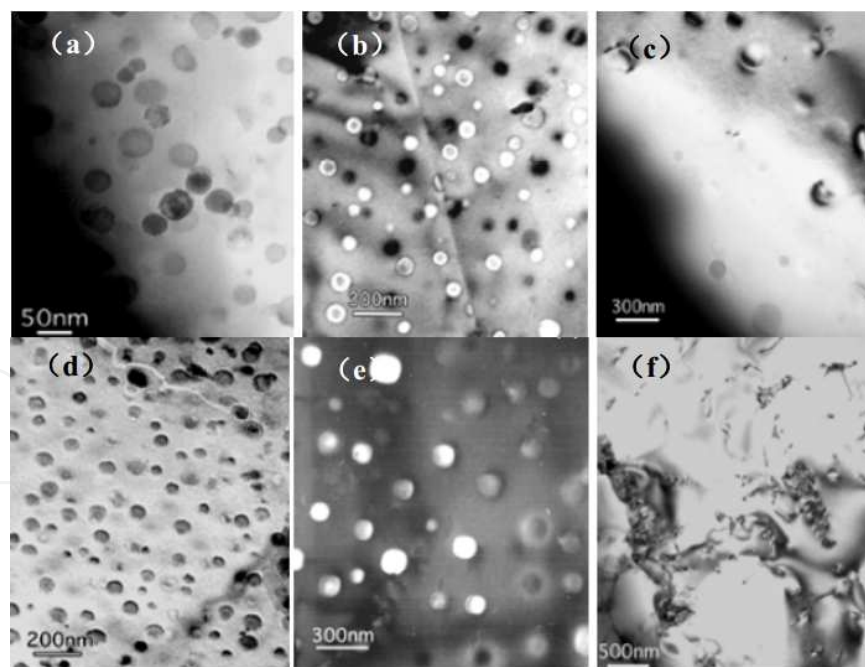


**Figure 16.** TEM images of CCA617 alloy aged at 700 °C/1000 h (a), 750 °C/1000 h (b), 800 °C/1000 h (c), 700 °C/3000 h (d), 750 °C/3000 h (e) and 800 °C/3000 h (f).

Figure\_17a shows the dispersively precipitated fine  $\gamma'$  ( $23\pm 4$  nm) at 750 °C, 50 h aging. These dispersively precipitated fine  $\gamma'$  particles coagulate to a larger size ( $68\pm 20$  nm) at 850 °C for

50h aging as shown in Figure\_17b. The TTT diagram of Nimonic 263 is clearly shown in Figure\_17c. It can be learned from this diagram that the basic structure for Nimonic 263 is mainly fine  $\gamma'$  precipitation in Ni-Cr-Co-Mo  $\gamma$ -matrix and carbide  $M_{23}C_6$  distributed at grain boundaries. It can be seen also from this TTT diagram that the  $Ni_3Ti$  type  $\eta$  phase can be formed at high temperature long time aging. The Ti-rich  $\gamma'$ -  $Ni_3(Al, Ti)$  in Nimonic 263 is a meta-stable precipitated phase for good strengthening effect. However the meta-stable Ti-rich type  $\gamma'$  phase will transform to a stable  $Ni_3Ti$  type  $\eta$  phase for long time aging at high temperature [21, 22].

Figure\_18 shows the very large plate-like  $\eta$  phase formation in Nimonic 263 after long time aging at high temperature [21].

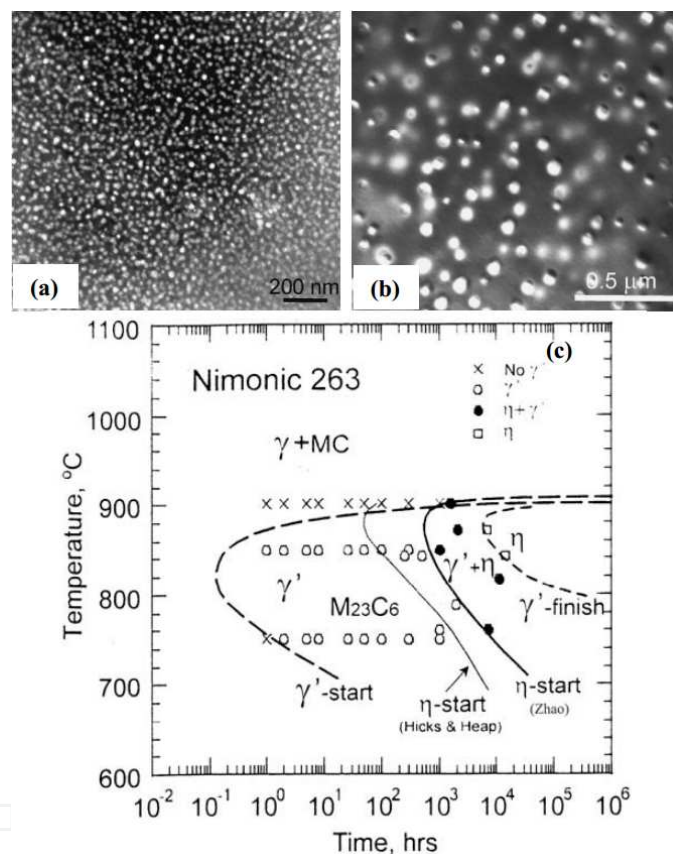
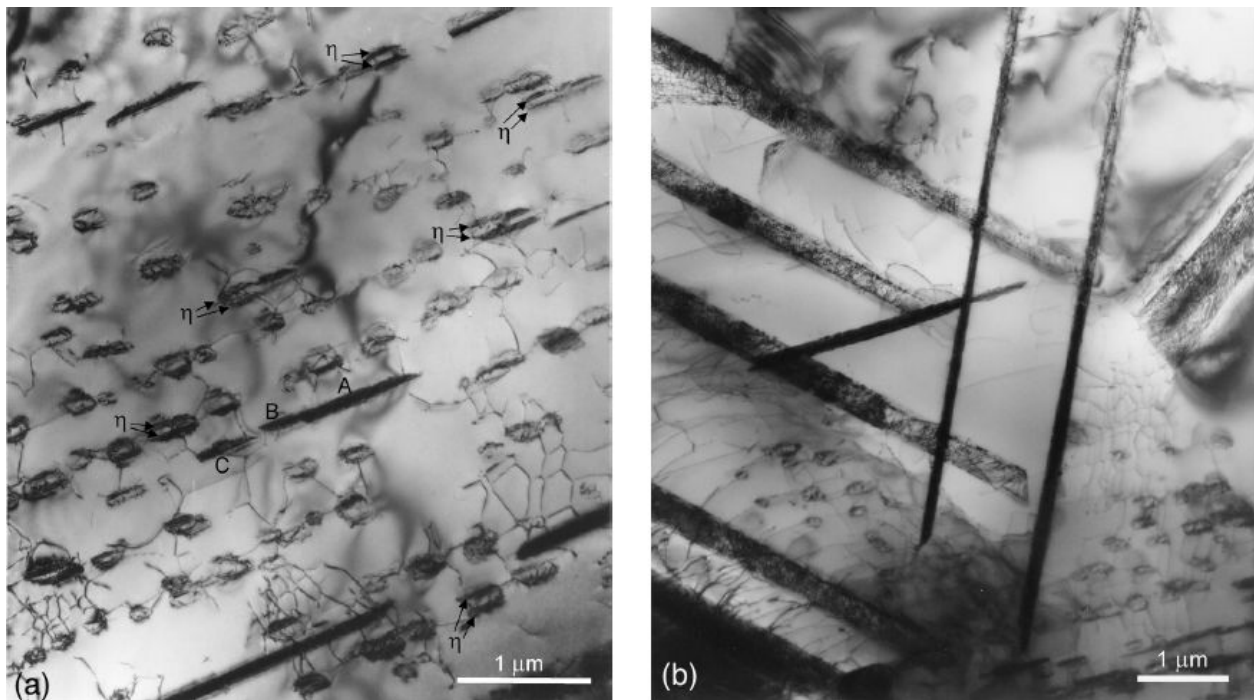


Figure 17. TEM dark field images of Nimonic263 aged at 750 °C (a) and 850 °C (b) for 50 h and TTT curve (c).

Nimonic 263 has been adopted as a good high stress rupture strength and good corrosion resistant Ni-base superalloy in aero-engines for not very long service time ( $\sim 10^3$ - $10^4$  h). However the fossil power plant should be put in service for a very very long time such as 30-40 years. The long time structure stability is a critical issue for superheater and reheater tubing application in 700 °C A-USC boiler.

Phase diagram calculation by Thermo-Calc can help us to understand the phase stability in the different temperature ranges. As the equilibrium phase diagram of Nimonic 263 (Figure\_19) shows that the  $\eta$ ,  $\sigma$  and  $\mu$  phase can be formed in different temperature ranges [23].





**Figure 18.** The TEM images of arranged  $\gamma'$  phase transformed to  $\eta$  phase after heat treatment at 800 °C for 8 h then aged at 900 °C for 1250 h (a) and dislocations distribution at  $\eta/\gamma'$  boundaries (b).

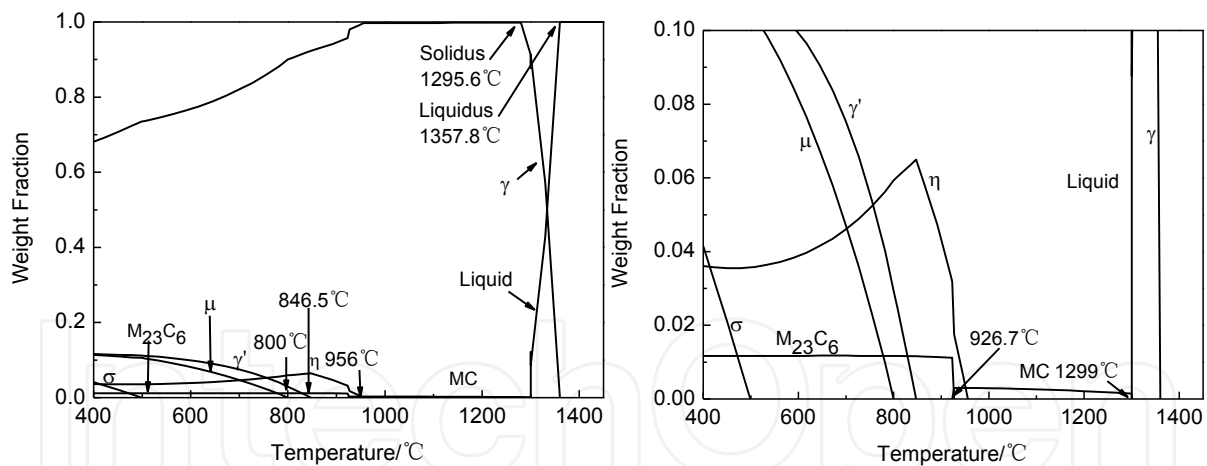


**Figure 19.** Phase diagram of Nimonic 263 calculated by Thermo-Calc.

It is clearly seen that except  $\gamma'$ ,  $\eta$  and  $\mu$  phase can be formed in a wide range of high temperatures. Figure\_20 is an example that a big amount of large plate-like  $\text{Ni}_3\text{Ti}$  type  $\eta$  phase formed after stress rupture test at 775 °C, 115 MPa for 12601 h [23]. It is clearly that strengthening effect of  $\gamma'$  is decreased dramatically by the transformation from  $\gamma'$  to  $\eta$ . It means that the structure stability of Nimonic 263 should be improved for 700 °C A-USC boiler superheater and reheater tubing components at very long time service.

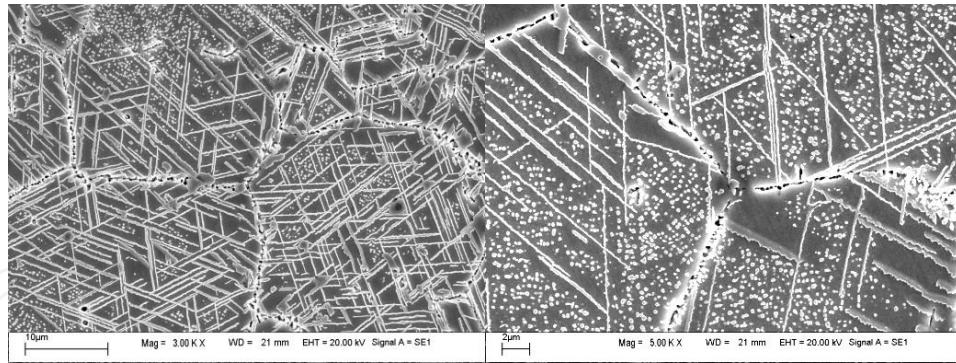


Figure 20. Microstructure instability of Nimonic 263 after the stress rupture test at 775 °C, 115 MPa of 12601 h.

## 2.6. Haynes 282 (Ni-20Cr-10Co-8.5Mo-2.1Ti-1.5Al-0.06C)

Haynes 282 was developed by Haynes International, USA in 2005. It is a corrosion resistant and high creep strength Ni-base superalloy. The original purpose for Haynes 282 is to develop a weldable Ni-base superalloy to replace Waspaloy for making different components in aero-engine industry. As today's knowledge understanding the Waspaloy is a good Ni-base superalloy in the intermediate temperature range for aero-engine application. However it is difficult for flat product and especially is almost cannot be welded for required components [24].

With 57%Ni, 20%Cr, 10%Co and 8.5%Mo for solid solution strengthening and 2.1%Ti, 1.5%Al for forming  $\gamma'$  precipitation strengthening. Haynes 282 falls into a subcategory within the larger category of the familiar  $\gamma'$  strengthened superalloys.

Phase diagram calculation result of Haynes 282 by Thermo-Calc is shown in Figure\_21 [25]. It can be seen that except the  $\gamma'$  precipitation possibly  $\mu$  phase and occasionally  $\sigma$  phase can be also formed in a certain temperature range. The carbides MC,  $M_{23}C_6$  and  $M_6C$  with a small amount should be existed in Haynes 282. The basic structure of Haynes 282 at as heat treated condition is about 17%  $\gamma'$  dispersively distributed in  $\gamma$ -matrix with grain boundaries precipitated carbides  $M_{23}C_6$  (0.67%),  $M_6C$  (0.05%) and also MC (0.16%) randomly distributed in  $\gamma$ -matrix [26].

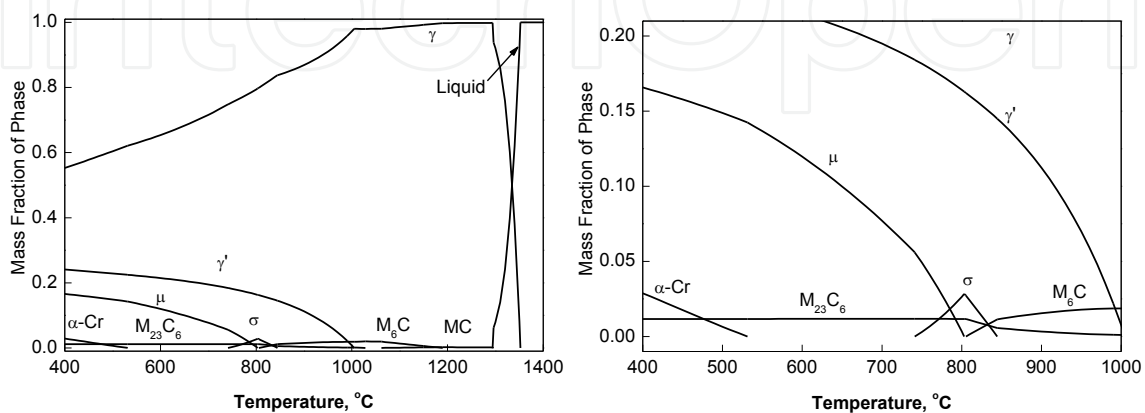


Figure 21. Phase diagram of Haynes 282 calculated by Thermo-Calc.

Figure\_22 shows the typical structure after long time aging at 649 °C, 760 °C and 816 °C for 1000 h [27]. These SEM images show that Haynes 282 characterizes with good structure stability. It still keep a structure with fine  $\gamma'$  precipitation in  $\gamma$ -matrix and carbides ( $M_{23}C_6$  and  $M_6C$ ) distribute at grain boundaries. The harmful phases such as  $\mu$  and  $\sigma$  have not been found yet.

Figure\_23 clearly shows that the tensile yield strengths of Haynes 282 after very long time aging at high temperatures are much higher than Haynes 230 Ni-base alloy [27].

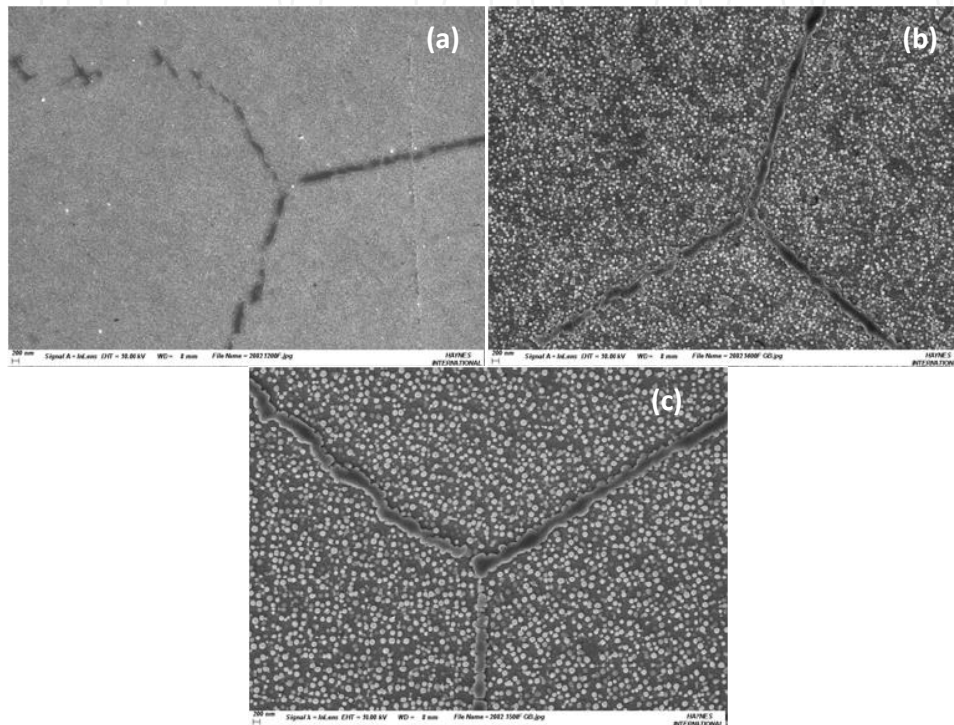


Figure 22. SEM images of Haynes282 aged at 649 °C (a), 760 °C (b) and 816 °C (c) for 1000 h.

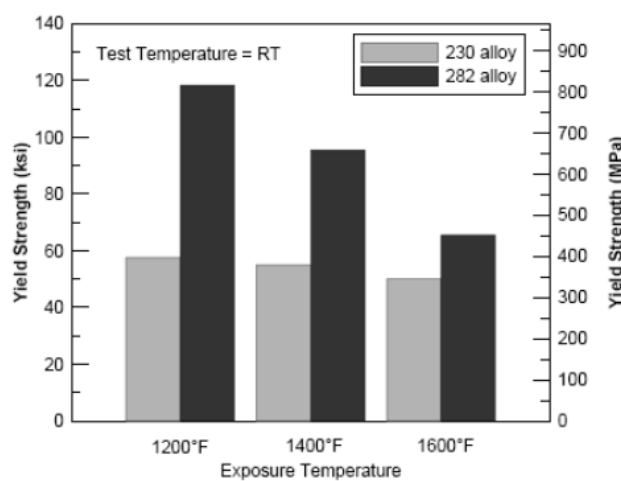


Figure 23. Comparison of room temperature tensile properties between Haynes282 (after 16,000 h aging) and Haynes230 alloy (after 20,000 h aging)



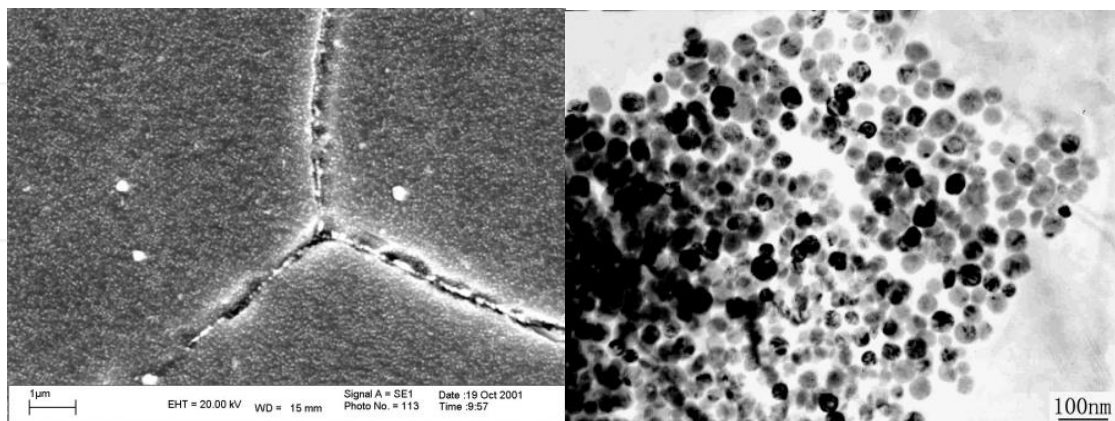
Furthermore the high temperature stress rupture strength of Haynes282 is also a little higher than Inconel 740, as the dash line indicated in Figure\_3. However Haynes International are just developing 282Alloy for 700 °C A-USC boiler superheater and reheater tubing application. Haynes will accumulate the important data together from seamless tube product for asking ASME Code in the future.

## 2.7. Inconel 740 (Ni-25Cr-20Co-0.5Mo-2Nb-1.9Ti-0.8Al-0.03C)

As above mentioned all Ni-Fe and Ni-base superalloys such as HR6W, GH2984, Haynes 230, Inconel 617/617B, Nimonic 263 (see Table 1) can not meet 700 °C A-USC boiler superheater and reheater tubing requirement (see Figure\_3 and 4).

Inconel 740, a new Ni-Cr-Co-Mo-Nb-Ti-Al superalloy, is developed in the year of 2000 by Special Metal Corp.(SMC, Huntington) USA for European THERMIE AD700 A-USC project with steam parameters of 700 °C, 35 MPa [28]. At this condition the superheater and reheater fire-side metal temperature can be 750-760 °C even higher. As we mentioned that the superheater and reheater require stress rupture strength(100 MPa, 10<sup>5</sup>h) at temperatures 750-760 °C, together with the high corrosion resistance(≤1 mm cross-section loss in 10<sup>5</sup> h). Inconel740 characterizes with the highest stress rupture strength and corrosion/oxidation resistance among today's commercial available candidate materials and can meet above mentioned strict requirements.

Typical microstructure and phase fraction of Inconel740 at standard heat treatment are shown in Figure\_24. The main strengthening phase  $\gamma'$  (12.98%) homogeneously distributes in Ni-Cr-Co  $\gamma$ -matrix,  $M_{23}C_6$  carbide (0.115%) and a very small amount(0.054%) of high Si-containing G-phase mainly precipitated at grain boundaries and MC-(Nb.Ti)C (0.183%) carbide formed at solidification process randomly distributes in the alloy.



Phase	$\gamma'$	MC	$M_{23}C_6$	G
wt%	12.980	0.183	0.115	0.054

**Figure 24.** Typical microstructure and phase fractions of Inconel 740 after standard heat treatment.

The microstructure of Inconel 740 is quite stable at 700 °C long time aging as shown in Figure\_25. However, it is quite different at 760 °C long time aging. There are a lot of plate-like  $\eta$ -phase nearby grain boundaries and rapidly grow to the grains. Moreover the large globular high Si-containing G phase distributed at grain boundaries as determined by EDAX(see Figure\_26) [29,30].

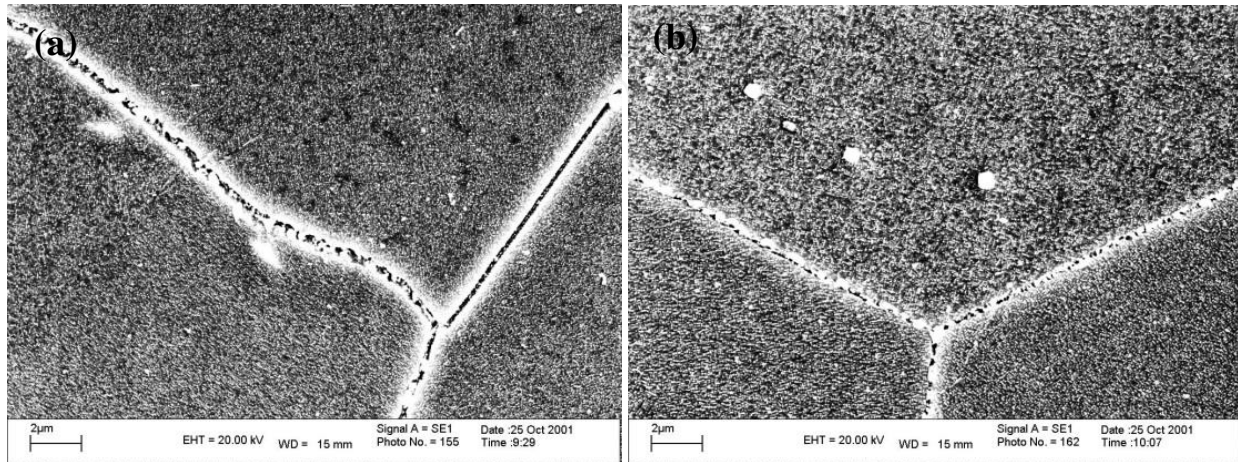


Figure 25. Stable microstructure of Inconel 740 at 704 °C long time aging: (a) 704 °C/1000 h and (b) 704 °C/2000 h.

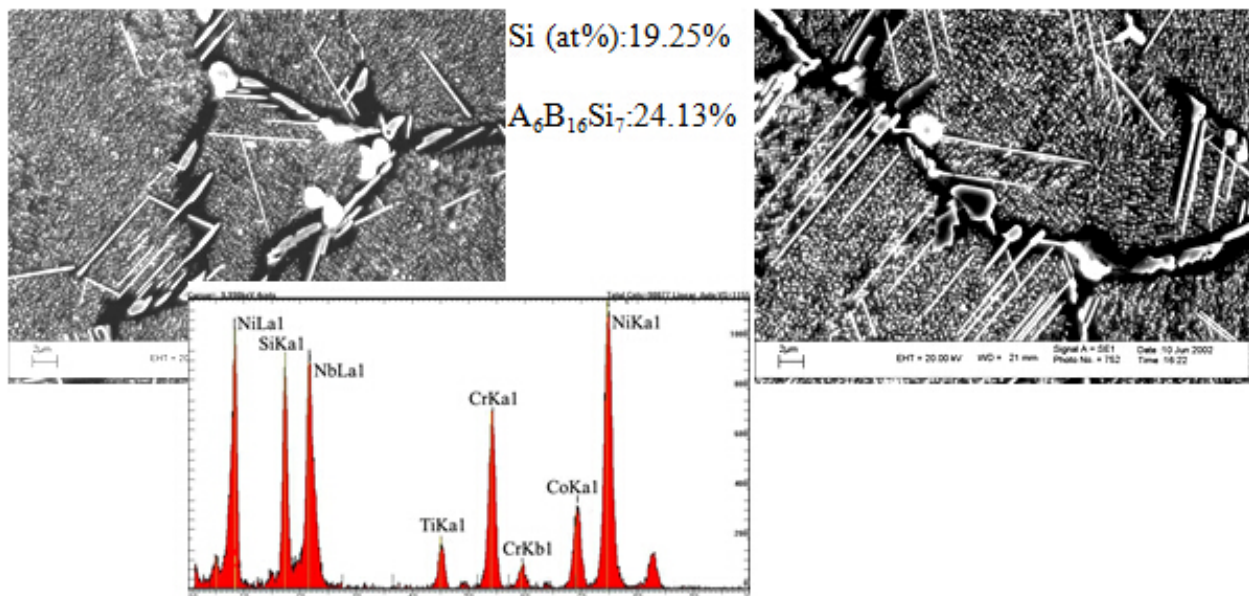
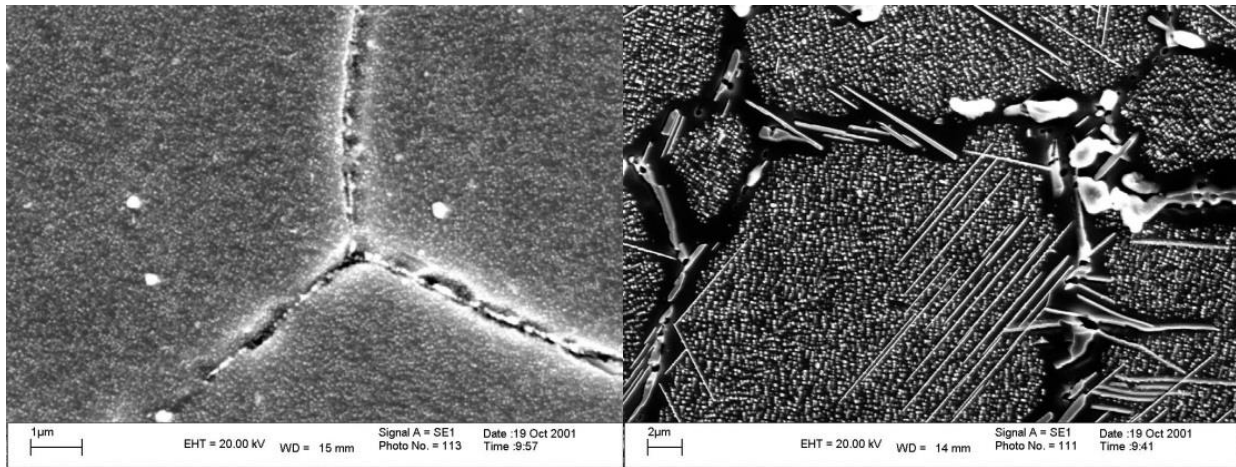


Figure 26. The large amount of  $\eta$ -phase and G-phase in Inconel 740 after 760 °C long time aging.

Detail quantitative determination of brittle high Si-containing G-phase after 704-760 °C long time aging is shown in Figure\_27. It is very harmful for Inconel 740 that the amount of G phase(0.471%) after 2000 h aging at 760 °C is almost 10 times than the amount of G-phase(0.054%) as at standard heat treatment condition. Moreover the unstability of  $\gamma'$  strengthening phase and the formation of  $\eta$ -phase have been also detail studied as shown in Figure\_28 [31].





standard heat treatment

aged at 760 °C for 2000h

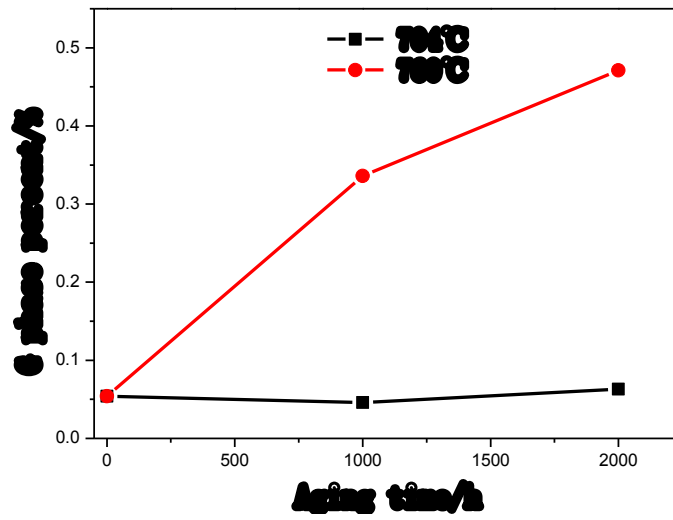


Figure 27. High Si-containing G-phase formation and plate-like  $\eta$ -phase precipitation in Inconel 740 at 760 °C long time aging.

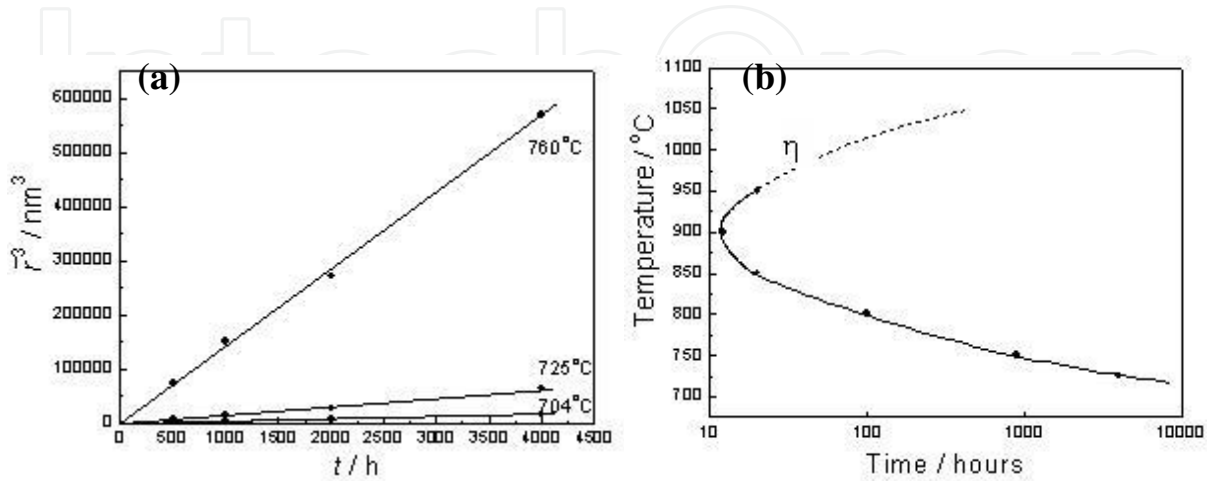


Figure 28. Coarsening of  $\gamma'$  phase(a) and the precipitation of  $\eta$ -phase(b) in Inconel 740.

It can be recognized that the structure stability is good for Inconel 740 during long time aging at the temperatures under 725 °C. The instability of Inconel 740 at 760 °C has been confirmed by 3 important factors: high coarsening rate of  $\gamma'$  phase, plate-like  $\eta$ -phase formation and high Si-containing brittle G-phase formation at grain boundaries. It will clearly develop degradation of strength and ductility both. Just for these reasons the structure stability improvement and modification of Inconel 740 for developing Inconel 740H should be done to fulfill the superheater/reheater requirements at the temperature 750 °C and above [32].

### 2.8. Inconel 740H (Ni-25Cr-20Co-0.5Mo-1.5Nb-1.35Ti-1.35Al-0.03C)

Inconel 740H is a modification of Inconel 740 for improvement of structure stability by the adjustment of Nb, Ti, Al and Si [33]. Chemical composition and phase fraction comparison between Inconel 740H and Inconel 740 is shown in Table 2 and 3 respectively. Figure\_29 shows the comparison of calculated phase diagrams of Inconel 740 and Inconel 740H. It can be seen from these results that the  $\gamma'$  strengthening phase is more stable in Inconel 740H than Inconel 740. The  $\eta$ -phase is eliminated in Inconel 740H and there is not existence of brittle high Si-containing G phase in Inconel 740H.

Alloy	C	Cr	Ni	Co	Mo	Nb	Ti	Al	Mn	Fe	Si
740	0.03	25	bal	20	0.5	2	1.8	0.9	0.3	0.7	0.5
740H	0.03	25	bal	20	0.5	1.5	1.35	1.35	0.3	0.7	0.15

Table 2. Chemical composition (wt%) comparison between Inconel 740H and Inconel 740.

Alloy	$\gamma'$	MC	$M_{23}C_6$	G
740	12.980	0.183	0.115	0.054
740H	14.623	0.220	0.202	0

Table 3. Phase fraction (wt%) comparison between Inconel 740H and 740.

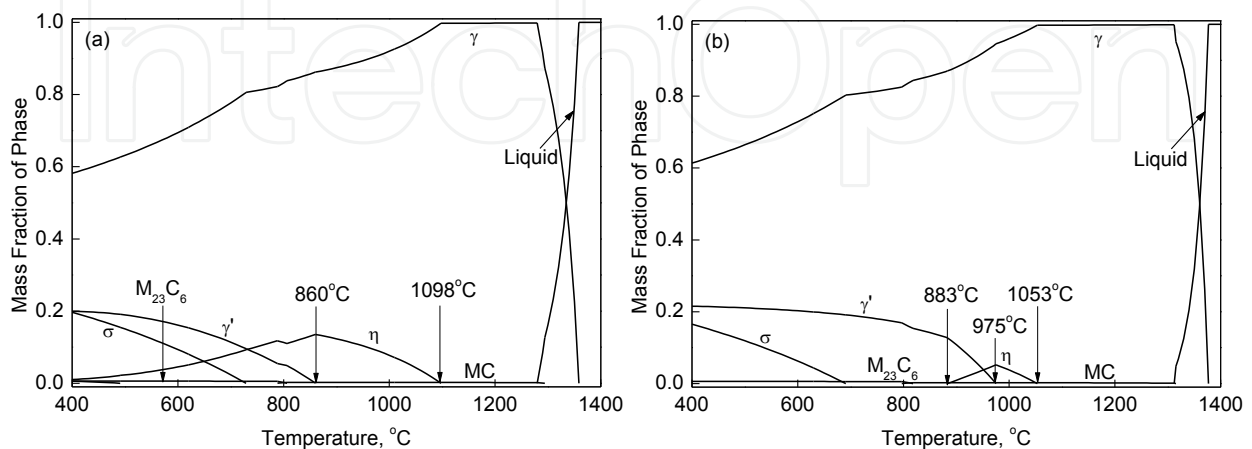


Figure 29. Phase diagram comparison between Inconel 740 (a) and Inconel 740H (b).

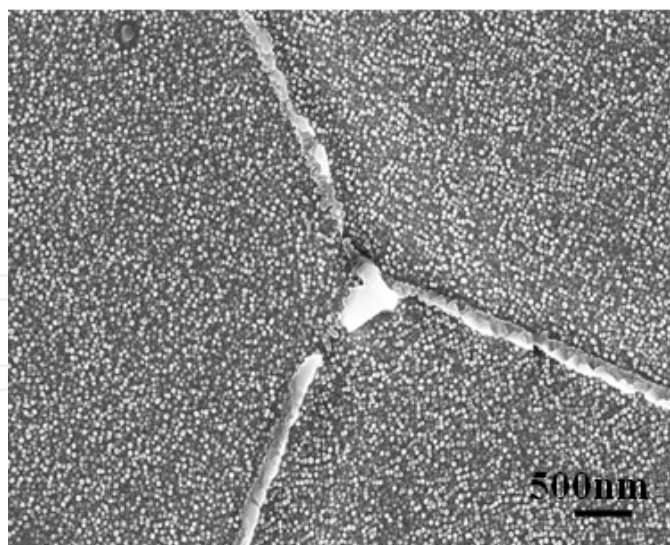


Figure 30. Typical microstructure of Inconel 740H after standard heat treatment.

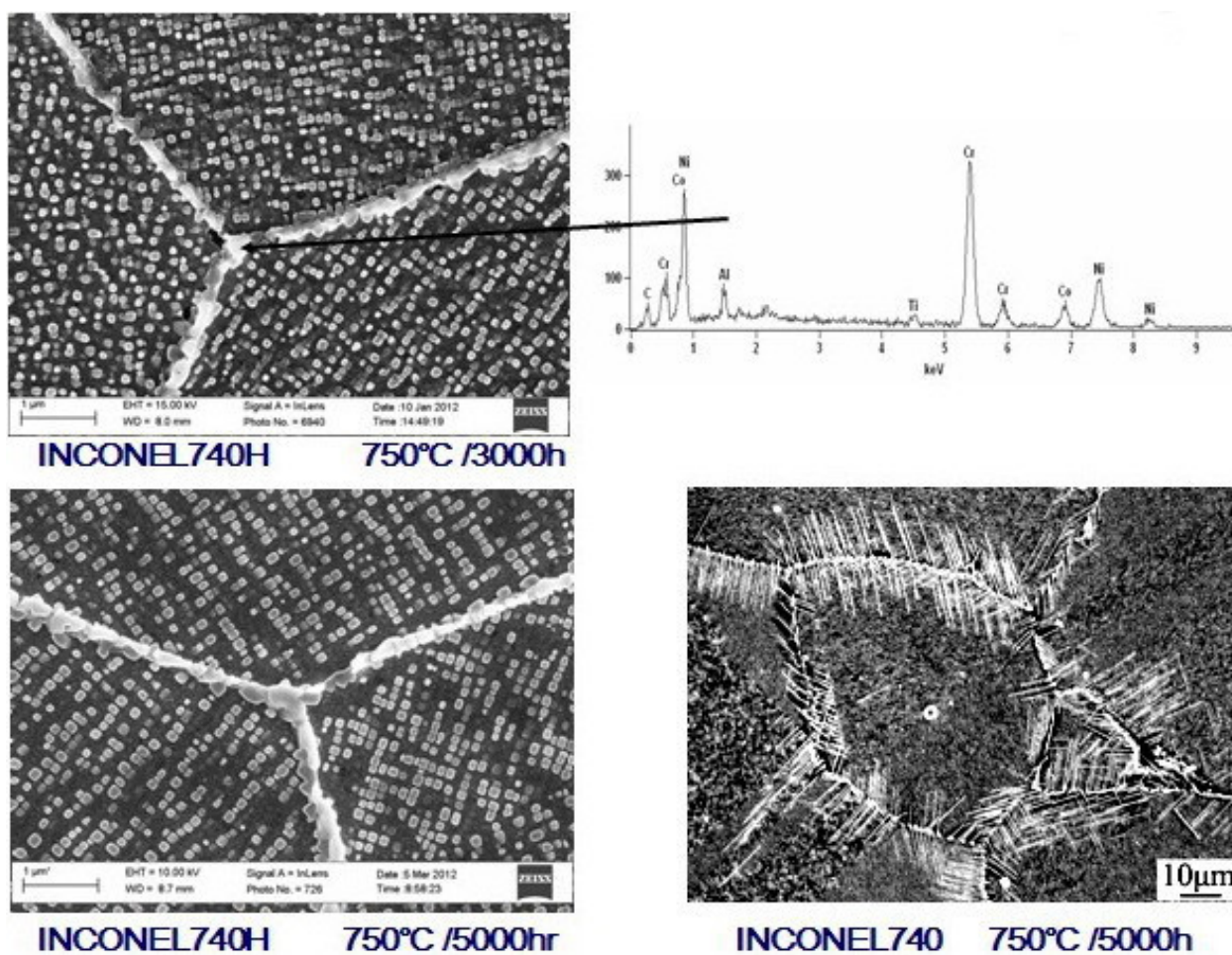


Figure 31. Long time structure stability comparison between Inconel 740H and 740 at 750 °C.



Typical microstructure of Inconel 740H after standard heat treatment as shown in Figure\_30 is very similar to the structure of Inconel 740 in comparison with Figure\_24. The main strengthening phase  $\gamma'$  (14.623%) homogeneously distributes in Ni-Cr-Co  $\gamma$ -matrix,  $M_{23}C_6$  carbide(0.202%) and also MC-(Nb,Ti)C carbide(0.220%) formed at solidification process randomly distributes in this alloy. However, the comparison of structure stability of Inconel 740H and Inconel 740 at 750 °C and 800 °C long time aging is quite different(see Figure\_31 and Figure\_32) [34]. Inconel 740H keeps stable  $\gamma'$  strengthening in Ni-Cr-Co  $\gamma$ -matrix and  $M_{23}C_6$  carbide at grain boundaries. However, plate-like  $\eta$ -phase formation and high Si-containing G-phase precipitation obviously happen in Inconel740. Moreover the  $\gamma'$  growth rate comparison between Inconel 740H and Inconel 740(see Figure\_33) clearly shows that Inconel 740H characterizes very good structure stability at 750 °C long time aging.

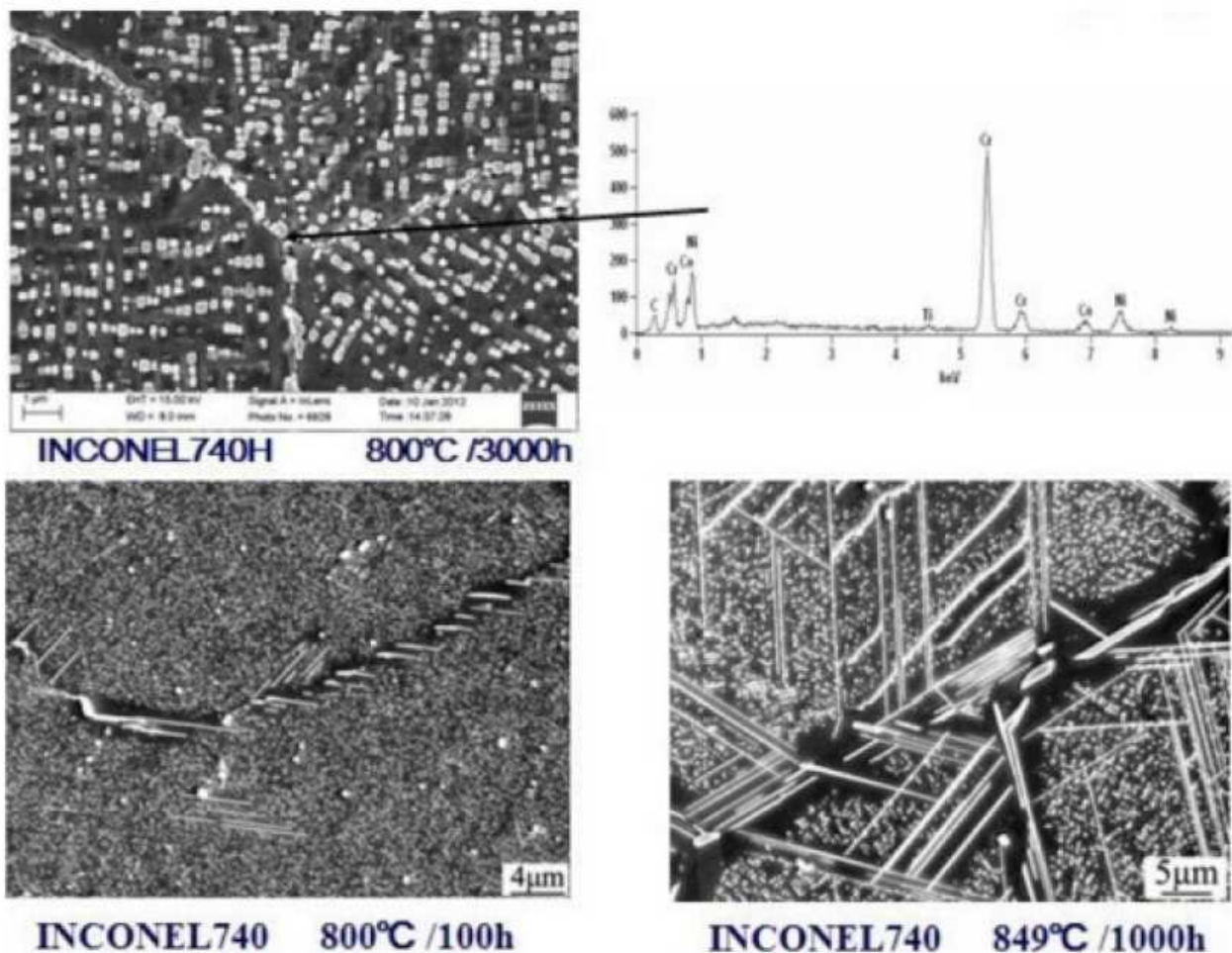


Figure 32. Long time structure stability comparison between Inconel 740H and 740 at 800 °C aging.

The structure stability study has been also conducted after high temperature stress rupture tests [30]. The structure of Inconel 740 sample tested at 775 °C, 170 MPa, after 2779 h shows a large amount of  $\eta$ -phase near grain boundaries and G phase formation at grain boundaries(see Figure\_34a). However, the structure of Inconel740H sample tested at 750 °C, 280 MPa, after

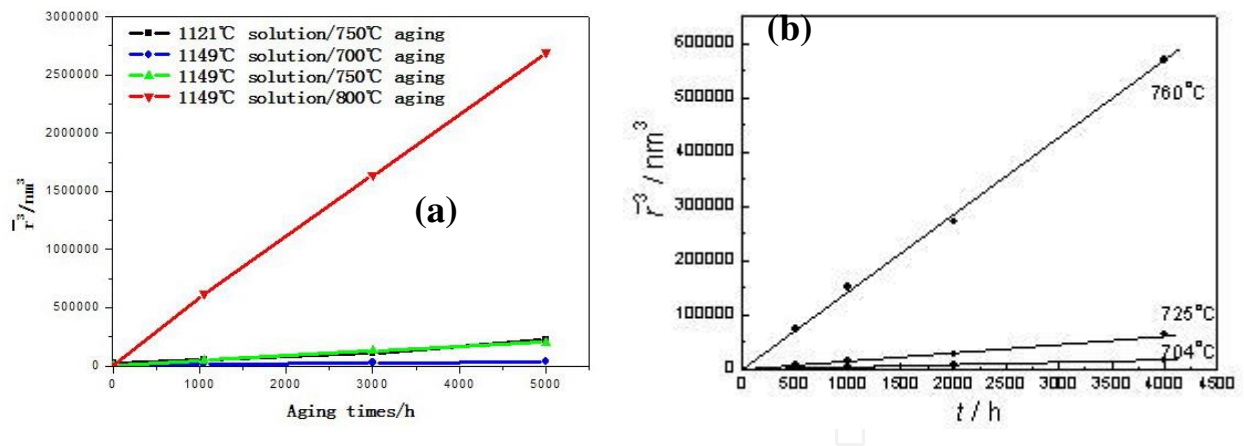


Figure 33.  $\gamma'$  growth rate comparison between Inconel 740H(a) and 740(b) at high temperatures.

1087 h still keeps stable  $\gamma'$  precipitation in  $\gamma$ -matrix and  $M_{23}C_6$  carbide distributed at grain boundaries and there are no existence of plate-like  $\eta$ -phase and brittle G-phase at grain boundaries(see Figure\_34b).

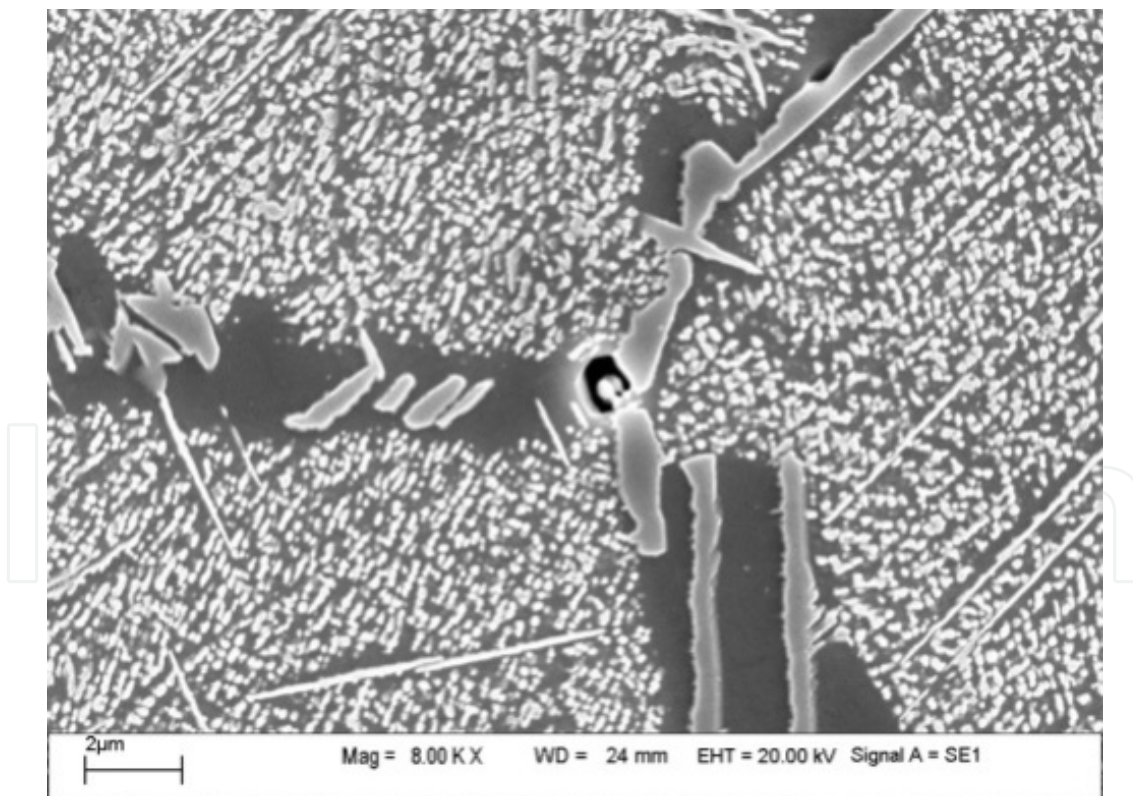


Figure 34. Microstructure comparison of Inconel740(a) and Inconel740H(b) stress rupture tested samples.

The impact toughness of Inconel 740H after high temperature long time aging is much higher than Inconel 740 as shown in Table 4.



Alloy	Exposure	CVN J/cm <sup>2</sup>
740	0 h	45
	750 °C-2000h	13.6
740H	0h	90.6
	700 °C-1050 h	29.5
	750 °C-1000 h	35.7
	800 °C-1000 h	50.5
	700 °C-3042 h	23.3
	750 °C-3000 h	29.8
	800 °C-3000 h	46.2
	700 °C-5000 h	34.7
	750 °C-5000 h	23.8
	800 °C-5000 h	45.3
	solution treatment at 1121 °C	93.7
	750 °C-1000 h(solution treatment at 1121 °C)	51.2
	750 °C-3000 h(solution treatment at 1121 °C)	44.4
	750 °C-5000 h(solution treatment at 1121 °C)	45.2

**Table 4.** Impact toughness comparison of Inconel 740H and Inconel 740 after high temperature long time aging.

### 3. Summary

A brief review of some candidate Ni-Fe and Ni-base superalloys for 700 °C A-USC fossil power plant application have been discussed. However up to now still have no success to build a 700 °C A-USC model plant, because high temperature materials test has not successfully passed at any 700 °C A-USC test beds.

One more issue must be mentioned that welding is very important for boiler tubing component making. Furthermore the thick wall pipe welding for header and main steam piping is more critical for building a power plant.

From the view point of high temperature stress rupture strength and corrosion/oxidation resistance among above mentioned Ni-Fe and Ni-base superalloys with ASME Code as indicated in Table 1. Inconel 740H may be a perspective high temperature material for 700 °C A-USC Project. However the weldability of Inconel 740H is still an important factor for real application.

Except today's commercial available Ni-Fe and Ni-base superalloys as listed in Table 1, some new Ni-Fe base and Ni-base superalloys are still developing in the world for 700 °C A-USC

Project. We hope that in close cooperation of world materials scientists and engineers the high temperature materials for 700 °C A-USC technology will be developed and put in a model power plant for long time service in the future.

## Author details

Xishan Xie<sup>1\*</sup>, Yunsheng Wu<sup>1</sup>, Chengyu Chi<sup>2</sup> and Maicang Zhang<sup>1</sup>

\*Address all correspondence to: xishanxie@mater.ustb.edu.cn

1 High Temperature Materials Research Laboratories, University of Science & Technology Beijing, Beijing, China

2 CPI Nuclear Power Institute, China Power Investment Corporation, Beijing, China

## References

- [1] Chi C Y, Yu H Y, Xie X S: Research and development of austenitic heat-resistant steels for 600 °C superheat/reheater tubes of USC power plant boilers. *World Iron & Steel*. 2012; 04: 50-65. DOI:10.3969/j.issn.1672-9587.2012.04.008
- [2] Viswanathan R, Henry J F, Tanzosh J: US program on materials technology for ultra-supercritical coal power plants. *Journal of Materials Engineering and Performance*. 2005; 14(3): 281-292. DOI: 10.1361/10599490524039
- [3] Robert Romanosky. *Global Advanced Fossil-Gen Summit*. 2011, Shanghai, China.
- [4] Guo J T, Du X K: A superheater tube superalloy GH2984 with excellent properties. *Acta Metallurgica Sinica*. 2005; 11: 1221-1227.
- [5] H. Semba, H. Okada, M. Yonemura: 34th MPA-Seminar Materials and Components Behaviour in Energy & Plant Technology, 2008. Stuttgart, Germany, 14.1-14.8.
- [6] Xie X S, Chi C Y, Zhao S Q: Superalloys and the development of advanced ultra-supercritical power plants. *Materials Science Forum*. 2013; 747: 594-603. DOI: 10.4028/www.scientific.net/MSF\_747-748.594
- [7] Baker B A, Smith G D: Corrosion resistance of Alloy 740 as superheater tubing in coal fired ultra supercritical boilers. *CORROSION 2004*. NACE International, 2004.
- [8] Shingledecker J P, Evans N D: Creep-rupture performance of 0.07 C–23Cr–45Ni–6W–Ti, Nb austenitic alloy (HR6W) tubes. *International Journal of Pressure Vessels and Piping*. 2010; 87(6): 345-350. DOI: 10.1016/j.ijpvp.2010.03.011
- [9] Igarashi M, Semba H, Yonemura M: Advances in materials technology for A-USC power plant boilers. *Advances in Materials Technology for Fossil Power Plants: Pro-*

ceedings from the Sixth International Conference, August 31-September 3, 2010, Santa Fe, New Mexico, USA. ASM International, 2011, 1022300: 72.

- [10] Semba H, Okada H, Yonemura M: In Proceeding of 34th MPA-Seminar. Stuttgart, 2008.
- [11] Guo J T, Zhou L Z, Yuan C: Microstructure and properties of several originally invented and unique superalloys in China. *The Chinese Journal of Nonferrous Metals*. 2011; 02: 237-250.
- [12] Wang S H, Du X K, Guo J T: Anticorrosion performance of GH984 alloy under various environmental conditions. *Corrosion Science and Protection Technology*. 2002; 05: 284-287.
- [13] Wang S H, Du X K, Zhao J F: Study of Al, Ti, Nb contents of GH984 alloy used in superheater tube of naval vessels. *Materials for Mechanical Engineering*. 1999; 02: 36-39.
- [14] Twancy H M: High-temperature oxidation behaviour of a wrought Ni-Cr-W-Mn-Si-La alloy. *Oxidation of Metals*. 1996; 45: 323-348.
- [15] Boehlert C J, Longanbach S C: A comparison of the microstructure and creep behaviour of cold rolled Haynes 230 alloy and Haynes 282 alloy. *Materials Science and Engineering A*. 2011; 528: 4888-4898.
- [16] Li J, Rui H, Hong C K: The effect of M<sub>23</sub>C<sub>6</sub> carbides on the formation of grain boundary serrations in a wrought Ni-based superalloy. *Materials Science and Engineering A*. 2012; 536: 37-44. DOI:10.1016/j.msea.2011.11.060
- [17] Chatterjee S, Roy A K: Mechanism of creep deformation of Alloy 230 based on microstructural analyses. *Materials Science and Engineering A*. 2010; 527(29): 7893-7900. DOI: 10.1016/j.msea.2010.08.069
- [18] Lin F S, Xie X S, Zhao S Q: Selection of superalloys for super heater tubes of domestic 700°C A-USC boilers. *Journal of Chinese Society of Power Engineering*. 2011; 12: 960-968.
- [19] Wu Q, Song H, Swindeman R W: Microstructure of long-term aged IN617 Ni-base superalloy. *Metallurgical and materials transactions A*. 2008; 39(11): 2569-2585. DOI: 10.1007/s11661-008-9618-y
- [20] Wu Q Y. Microstructural evolution in advanced boiler materials for Ultra-Supercritical Coal power plants [thesis]. Cincinnati : University of Cincinnati; 2006.
- [21] Zhao J C, Ravikumar V, Beltran A M: Phase precipitation and phase stability in Ni-monic 263. *Metallurgical and Materials Transactions A*. 2001; 32(6): 1271-1282. DOI: 10.1007/s11661-001-0217-4
- [22] Hicks B, Heap M: Report No, B48749, Lucas Gas Turbine Equipment Ltd., Materials Laboratory, Burnley, Sept. 25, 1968.

- [23] Xie X S Dong J X, Wang J: Structure Stability Analyses on Nimonic 263 after Long Time Stress Rupture Tests (internal report). High Temperature Materials Research Laboratories, University of Science & Technology Beijing, 2011.
- [24] Pike L M: Development of a fabricable gamma-prime strengthened superalloy. Haynes International. 1020: 46904-9013.
- [25] Liu J Q, Zeng Y P, Xie X S: Thermodynamic simulation calculation of precipitation phase in a new-type Ni-based superalloy. *Materials Review*. 2007; 09: 119-122.
- [26] Zeng Y P, Liu J Q, Xie X S: Microstructure and properties analysis of a new wrought superalloy. *Acta Metallurgica Sinica*. 2008; 05: 540-546.
- [27] Pike L M: Long term thermal exposure of Haynes 282 alloy. *Superalloy 718 and Derivatives*, 2010: 644-660. DOI: 10.1002/9781118495223.ch50
- [28] Special Metals Corporation. Inconel740 bulletin. Special Metals Corporation, Huntington, WV, USA, 2005.
- [29] Zhao S Q, Xie X S: Properties and microstructure after long term aging at different temperatures for a new nickel base superalloy. *Acta Metallurgica Sinica*. 2003; 04: 399-404.
- [30] Zhao S Q, Xie X S, Smith G D: Microstructural stability and mechanical properties of a new nickel-based superalloy. *Materials Science and Engineering A*. 2003; 355(1): 96-105. DOI: 10.1016/S0921-5093(03)00051-0
- [31] Zhao S Q, Dong J X, Xie X S: Thermal stability study on a new Ni-Cr-Co-Mo-Nb-Ti-Al superalloy. *Proceedings from the 10th International Symposium on Superalloy*. 2004: 19-23.
- [32] Xie X S, Zhao S Q, Dong J X: An investigation of structure stability and its improvement on new developed Ni-Cr-Co-Mo-Nb-Ti-Al superalloy. *Materials Science Forum*. 2004; 475: 613-516.
- [33] Xie X S, Zhao S Q, Dong J X: A new improvement of inconel alloy 740 for USC power plants. *Proc of Advances in Materials Technology for Fossil Power Plants*, ASM, 2008.
- [34] Chi C Y, Zhao S Q, Lin F S: High Temperature Long-term Structure Stability Study on Inconel740/740H Ni-Base Superalloy. Keynote Lecture at Proc of The 5th Symposium on Heat Resistant Steels and Alloys for High Efficiency USC/A-USC Power Plants 2013, Seoul, Korea, 2013.